Soft Matter

Cite this: *Soft Matter*, 2011, **7**, 5826

www.rsc.org/softmatter

PAPER

Unequal stoichiometry between crosslinking moieties affects the properties of transient networks formed by dynamic covalent crosslinks†

Julie I. Jay,[a] Kristofer Langheinrich,[b] Melissa C. Hanson,[b] Alamelu Mahalingam[a] and Patrick F. Kiser*[ab]

Received 9th February 2011, Accepted 7th April 2011
DOI: 10.1039/c1sm05209h

A pH responsive system capable of forming a self-healing transient network across the pH 4.5 to 7.5 range is developed by increasing the ratio of phenylboronic acid (PBA) moieties to salicylhydroxamic acid (SHA) moieties incorporated in poly[*N*-2-hydroxypropyl]methacrylamide polymer backbones. We used particle tracking to assess network formation across the pH range of 4.5 to 7.5 with PBA : SHA stoichiometry of reactive groups of 1 : 1, 5 : 1 and 10 : 1. The 10 : 1 ratio of PBA : SHA forms a transient network across the entire pH range, while the 1 : 1 PBA : SHA materials demonstrate more liquid like behavior at pH 4.5 and forms a transient network only at neutral pH. At pH 7.5 increasing the ratio of PBA to SHA from 1 : 1 to either 5 : 1 or 10 : 1 increases the $G'_{plateau}$ sixty-fold, indicating that the higher probability of crosslink formation impacts the density of crosslinks compared to a 1 : 1 ratio of PBA to SHA. Above pH 5.5 the 5 : 1 and 10 : 1 PBA : SHA gels behaved similarly. Over the temperature range of 10 to 55 °C, the unequal stoichiometric ratios of 10 : 1 and 5 : 1 PBA : SHA transient networks behave similarly, with $G'_{plateau}$ dropping with a corresponding decrease in the characteristic relaxation time. Master curve analysis demonstrates superposition of the 1 : 1, 5 : 1 and 10 : 1 PBA : SHA stoichiometry except under the weakest network conditions (low pH, high temperature) suggesting that the same crosslinking mechanism dominates the network behaviour. The simple and complex viscosity is compared as a function of pH with shear thickening behaviour observed below pH 5.5. The 10 : 1 PBA : SHA crosslinked-network displays self-healing properties after repeated break cycles at both pH 4.5 and pH 7.5 demonstrating that increasing the ratio of PBA to SHA provides a material that can form a self-healing transient network at low pH, where the PBA–SHA crosslink association is weak, to neutral pH where the PBA–SHA complex is stabilized.

Introduction

Modifying the crosslinking interactions between polymer chains is an obvious target to modify the structure–property relationships in network polymers. If the crosslinking reaction is reversible it is possible to chemically manipulate the crosslinking interaction to provide modulation of the viscoelastic properties as well as the ability to create materials that self-heal in response to mechanical stress. Most reversible hydrogel systems are designed to rapidly recover after exposure to high shears or stresses and have relied on hydrogen-bonding, electrostatic interactions and/or the hydrophobic effect.[1–4] The use of reversible covalent crosslinks has not been broadly applied to hydrogel engineering even though one of the interesting behaviors of materials constructed with this variety of crosslinks is the ability to self-heal.[5–11] The dynamic nature of these reversible crosslinked systems makes them difficult to categorize. In common usage the word 'gel' can refer to both viscoelastic fluids (*e.g.* hair gels and semisolid pharmaceutical formulations) and covalently crosslinked polymer networks. In this work we will use the naming conventions inspired by Russo where dynamic self-healing polymeric structures are referred to as 'transient networks' and networks that do not heal or flow as 'solid networks' or gels.[12]

We have studied pH responsive polymer networks based on the pH sensitive, dynamic covalent crosslink formed from phenylboronic acid (PBA) and salicylhydroxamic acid (SHA). Boronate–diol complexes are reversible because of the rapid hydrolysis that occurs when the boronate is in its trigonal conformation compared to its more stable tetrahedral form. The equilibrium between the trigonal and tetrahedral conformation depends on the pH and the diol.[13] The PBA–SHA complex is unique in its ability to exist in the more stable tetrahedral boronate conformation even at slightly acidic pH values[14,15] compared to other diol complexes in which PBA predominantly exists in its tetrahedral configuration only at alkaline pH.[13] Our studies were based on linear polymers using the water soluble, biocompatible polymer backbone poly[*N*-2-hydroxypropyl]methacrylamide (pHPMAm)[16] functionalized with five

[a]*Department of Pharmaceutics and Pharmaceutical Chemistry, University of Utah, Salt Lake City, UT, 84112-5820, USA*
[b]*Department of Bioengineering, University of Utah, Salt Lake City, UT, 84112-5820, USA. E-mail: patrick.kiser@utah.edu*
† Electronic supplementary information (ESI) available. See DOI: 10.1039/c1sm05209h

or ten mole percent PBA or SHA (PBA_5–SHA_5 or PBA_{10}–SHA_{10}).[5,17] These polymers formed transient networks at acidic pH and solid networks at neutral pH.

However neither material was capable of recovery of the elastic modulus at neutral pH,[5] which reduces their potential use in physiological environments exposed to high stresses and shears at this pH. One approach we have probed to modulate the crosslinking interaction is locally adjusting the pH of the macromolecular boronate systems *via* the Donnan effect,[18,19] by utilizing a sulfate anionic polyelectrolyte backbone.[6] However, these polymers showed no temporary gel structure at acidic pH even at high salt concentrations. We are interested in engineering transient networks with this system that are self-healing, as defined by the recovery of the elastic modulus after exposure to high shear, viscoelastic fluids at physiological pH of 7.0 as well as at slightly acidic pH. At neutral pH the tetrahedral form of the PBA–SHA complex exists in equilibrium with a small amount of free PBA,[14,15] suggesting that some degree of reversibility at the level of a single crosslinker exists. Our previous investigations showed that at pH 5.5 HPMAm based PBA_5–SHA_5 materials were transient networks capable of self-healing at low strains, while PBA_{10}–SHA_{10} formed crosslinked solid networks.[5] This result indicates that the extent or number of crosslinks formed at a given pH impacts the material's self-healing properties.

We discovered that 1 mol% PBA or SHA functionalized HPMAm polymers formed self-healing PBA_1–SHA_1 transient networks at neutral pH. However, at pH 4.5 an extended transient network did not occur, likely due to the fact that the rapid hydrolysis of the PBA–SHA cyclic ester (see Scheme 1a) prevented the formation of the necessary number of crosslinks. Increasing the stoichiometry ratio of polymer-bound PBA to polymer-bound SHA amplifies the probability for formation of the PBA–SHA cyclic ester crosslink at acidic pH and thus for formation of a transient network. The lower mol% of SHA moieties restricts the number of stabilized PBA–SHA cyclic ester crosslinks capable of forming at neutral pH thus allowing for self-healing of the crosslinked polymer network after deformation at pH 7.5 (Scheme 1). In this paper we characterize for the first time how the use of an unequal ratio between the crosslinking moieties can move the self-healing transient network into the neutral pH range. We accomplish this by using 5 or 10 mol% PBA functionalized HPMAm polymers interacting with a 1 mol% SHA functionalized HPMAm polymer and show how unequal stoichiometry of the crosslinking moieties impacts the pH and temperature dependence of the viscoelasticity properties, the simple and complex viscosity, as well as the self-healing property of the resulting materials.

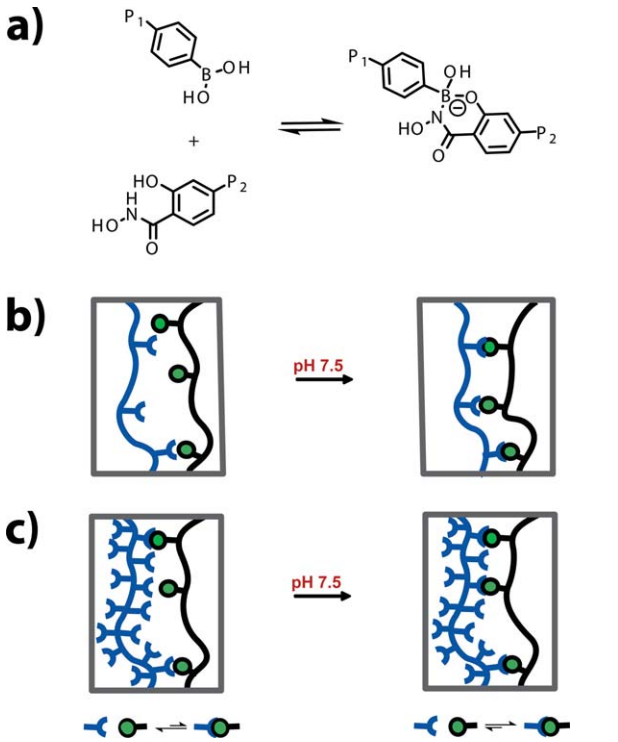

Scheme 1 (a) Scheme illustrating the equilibrium between reversible polymer-bound phenylboronate–salicylhydroxamate (PBA–SHA) crosslinks. (b) Self-healing viscoelastic transient networks are formed from PBA–SHA crosslinks above neutral pH (right) using a low, symmetric ratio of polymer-bound phenylboronic acid (PBA, blue) and polymer-bound salicylhydroxamic acid (SHA, green). However, the rapid hydrolysis of the reversible covalent PBA–SHA crosslink at slightly acidic pH (left) results in too few crosslinks—to create an extended network. (c) Increasing the ratio of polymer-bound PBA provides an increased probability for crosslink formation, and thus formation of a transient network at slightly acidic pH (left), while maintaining a maximum number of crosslinks at neutral pH to still provide a self-healing crosslinked network (right) as the equilibrium between the PBA–SHA crosslink shifts, becoming less susceptible to hydrolysis.

Materials and methods

Materials

The following materials were purchased from Sigma-Aldrich, Inc., St Louis, MO: methacryloyl chloride, sulfate modified polystyrene beads, and 2,2′-azobisisobutyronitrile (AIBN). AIBN was then recrystallized from chloroform in a chloroform–N_2(l) bath. All other chemicals and reagents were purchased from Aldrich or Acros and used without further purification unless otherwise noted. Dimethylformamide (DMF) and ethyl acetate were dried over 4 Å molecular sieves. Polymer molecular mass distributions were determined in deionized distilled water (DDI) or HPLC grade DMF using gel permeation chromatography (GPC) (HPLC 1100, Agilent Technologies) equipped with an aqueous column (PL aquagel-OH mixed, Polymer Labs) or an organic column (PLgel mixed-B, Polymer Labs), a differential refractive index detector (BI-DNDC, Brookhaven Instruments) and a multi-angle light scattering detector (BI-MwA, Brookhaven Instruments). All ^{1}H NMR spectra were acquired on a Varian Mercury 400 MHz spectrometer. Doubly deionized water was used in all experiments. For buffered samples the pH was adjusted with a Mettler Toledo Probe (Cole-Parmer) after 3 point calibration at pH 4, 7 and 10.

Monomer synthesis

The phenylboronic vinyl monomer, *N*-[3-(2-methyl-acryloylamino)-propyl]-4-amidophenylboronic acid (APMAmPBA), and the SHA vinyl monomer, 4-[(2-methyl-acryloylamino)-methyl]-salicylhydroxamic acid (MAAmSHA), were synthesized

according to the previously published protocols,[6] as was 2-hydroxypropylmethacrylamide (HPMAm).[17]

Polymer synthesis

Polymers were synthesized by free radical polymerization using 99 : 1, 95 : 5, or 90 : 10 mole ratios of HPMAm with APMAm–PBA and 99 : 1 mole ratios of HPMAm and MAAmSHA (Scheme 2). Polymerizations were performed using a 1 M monomer solution with 2,2′-azobisisobutyronitrile (AIBN, 0.6 mol%) in DMF 4 Å at 65 °C for 24 h under nitrogen atmosphere. Polymers were crudely purified through trituration into acetone. After the first trituration PBA-containing polymers were deprotected by acidifying with a 1 : 1 solution of methanol and aqueous 1 M HCl for 30 min at room temperature. Polymers were then lyophilized. Polymers were ultracentrifuged four times using Amicon Ultra-15 10K MWCO centrifuge tubes (Millipore) at a polymer concentration of 25 mg mL^{-1}. The first pass filtration was performed using 100 mM pH 7.5 PBS buffer and the next three purification passes used DDI water. Samples were centrifuged at 3000 rpm for 90 min followed by lyophilization. Actual molar feed ratios of polymers were determined in ^1H NMR in D_2O: PBA_1—2%; PBA_5—6%; PBA_{10}—10%; and SHA_1—1% (see Fig. S9–S12†). Mw Mn^{-1} was determined in HPLC grade DMF or DDI water by GPC: PBA_1—416/242 kDa; PBA_5—244/117 kDa; PBA_{10}—277/161 kDa; and SHA_1—121/84 kDa.

Dynamic rheology

Polymers were individually dissolved in buffer (100 mM acetate, MES, citrate or phosphate buffer) at 200 mg mL^{-1} concentrations. Any pH adjustments were performed with either 1 M HCl or 1 M NaOH before diluting to the final concentration. Mixtures were formed *in situ* by simultaneously pipetting 85 μL of PBA_1, PBA_5, or PBA_{10} with SHA_1 polymer solutions directly onto the rheometer's Peltier plate.

Dynamic rheology was performed using methods similar to those previously described using a cone-and-plate configuration on a stress-controlled rheometer (AR550, TA Instruments).[6] Briefly, a steel, 4° cone-shaped, 20 mm diameter geometry was used for all experiments with a total sample volume of 170 μL. Time sweeps were performed at 25 °C at a small amplitude oscillatory stress (1–10 Pa) and small angular frequency (5 rad s^{-1}) until the material's elastic modulus, G', plateaued for at least 15 min. The temperature was then raised to 37 °C and the material was allowed to equilibrate for 2 min. A second time sweep was conducted until G' plateaued for at least 15 min. For each new sample an oscillatory stress sweep was then performed (0.1–100 Pa oscillatory stress, 5 to 25 rad s^{-1} angular frequency) to determine the linear viscoelastic range from which an oscillatory stress was chosen and applied to all subsequent experiments at that condition. Oscillatory frequency sweeps were then performed at a controlled oscillatory stress (ranging from 5 to 30 Pa) determined from the linear viscoelastic region of oscillatory stress sweeps (0.01–100 rad s^{-1} angular frequency depending on the gel's crossover frequency characteristics). The same parameters were then used to determine frequency sweeps at 10 °C, 45 °C and 55 °C. Dynamic gel strength ($G'_{plateau}$) was calculated as the average G' from the plateau region of each oscillatory frequency sweep. For pH 7.5 PBA_1–SHA_1 where no defined plateau was exhibited, the G' plateau was determined by averaging the G' values beyond the frequency where G' equaled G''. The characteristic relaxation time, τ, was then calculated as:

$$\tau = 2\pi/\omega_c \quad (1)$$

where ω_c is the crossover frequency in rad s^{-1} and is determined from the angular frequency at which G' equals G''. All experiments were done in triplicate unless otherwise noted and data are represented as the mean. The complex viscosity, η^* (Pa s), was determined from the frequency sweeps.

The simple viscosity was measured using the same apparatus, geometry, and formulation as above for each sample. A steady state flow was applied with shear rates ranging from 0.01 to 100 s^{-1} at 10 °C, 25 °C, 37 °C, 45 °C and 55 °C depending on the sample.

To characterize the responsiveness of the materials from multiple stress-induced breakdowns, the material was allowed to come to equilibrium as determined by time sweeps at 37 °C at a small amplitude oscillatory stress (5–30 Pa) and small angular frequency (3–25 rad s^{-1}) until the material's elastic modulus, G', plateaued for at least 15 min. The mixture was then subject to a consecutive five to six break down and recovery cycles. Each cycle consisted of a two minute break, at an oscillatory stress chosen above the linear viscoelastic region where G' began to decrease (750–3000 Pa depending on the material) followed by a 60 min recovery at an oscillatory shear stress determined from the linear viscoelastic region and angular frequency from the plateau region of the frequency sweeps (5 to 30 Pa oscillatory stress and 3 to 25 rad s^{-1} angular frequency). The magnitude of oscillatory stress applied was determined from stress and recovery tests to ensure that values of the oscillatory stress did not result in the shear thinned material being spun out of the geometry.

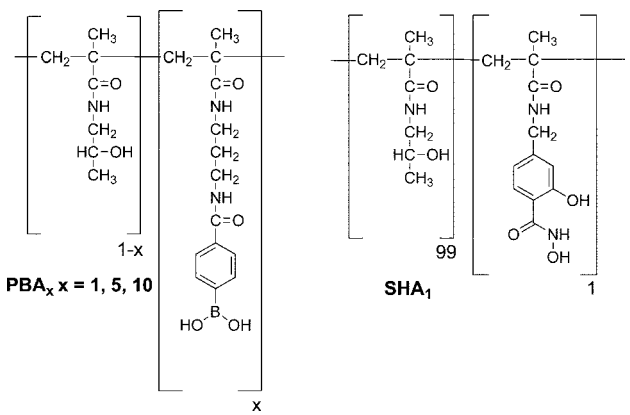

Scheme 2 Chemical structures of p(HPMAm-APMAmPBA) at 1, 5, and 10 mol% APMAmPBA (PBA_1, PBA_5 and PBA_{10}) respectively and p($HPMAm_{99}$-$MAAmSHA_1$) (SHA_1).

Particle tracking

The bead solutions of 100 nm sulfonated red fluorescent nanoparticles were prepared from a 2.5% stock (Sigma-Aldrich) and diluted to 0.162% in the appropriate buffer. 0.25 μL of the bead

solution was added to each polymer solution to give a final bead concentration of 0.002%. Materials were prepared by mixing 20 μL of the individual polymer solution (200 mg mL^{-1}) with 0.1 μL of the bead solution. The resulting material was removed with either a positive displacement pipette or a small spatula and placed at the center of a silicone sealed 5 mm well on a Bioptechs Delta T4 culture dish (0.17 mm) (Bioptechs Inc.) and topped with mineral oil to prevent evaporation. All imaging was done at 37 °C in a temperature controlled chamber. Three image stacks at different locations in the mixture were taken using a 60× oil immersion objective (NA 1.49) on a Nikon Eclipse Ti microscope and imaging system (Nikon Instruments Inc.) using NIS Elements Software. Images were collected at a scan speed of 15 images per second for a 512 × 512 pixel image. To minimize wall effects images were collected at least 50 μm into the material. Movies were converted to an 8 bit tiff stack using ImageJ (NIH).

The mean squared displacement (MSD, $\langle \Delta r(t)^2 \rangle$) of particles as a function of pH was measured by analyzing their trajectories at each experimental condition using IDL (ITT Visual Information Solutions) with particle tracking macros. Particle trajectories and the ensemble-averaged MSD were extracted using algorithms developed and kindly provided by Crocker and Grier,[20] and maintained by Eric R. Weeks. The ensemble-averaged MSD was determined from:

$$\langle r(t)^2 \rangle = \langle x(t)^2 - y(t)^2 \rangle \quad (2)$$

The experimentally determined two dimensional ensemble-averaged MSD can then be used to calculate the diffusion coefficient by fitting a line to the $\langle \Delta r(t)^2 \rangle$ versus t MSD plot to determine the slope and dividing it by four for 2-dimensional space.

Results and discussion

We are interested in new hydrogel crosslink chemistries to use in materials in the context of drug delivery and sexually transmitted infection (STI) prevention science.[21] Of particular interest to us is the development of pH responsive materials capable of sensing pH changes in the range of 4 to 7 by changing their network crosslink density, and therefore effective mesh size, to stop the movement of viral particles; much like the mechanism that mucins have in the GI and reproductive tract.[22] We are also interested in the ability of these pH responsive materials to self-heal due to exposure of shear rates up to 100 s^{-1} that could occur during *in vivo* use.[23]

The boronate–diol complex allows formation of pH responsive, reversible bonds that would allow us to engineer a material to meet these requirements. The PBA–SHA complex, unlike the majority of boronate–diol interactions, is able to form at slightly acidic pH.[24] In designing a material to act as a barrier to viral particles we selected this complex as our crosslink due to the pH change that occurs in the human vaginal lumen, from the slightly acidic precoital pH of vaginal fluid (pH 4–5) to neutral in the presence of semen.[25,26] Using the PBA–SHA complex we aim to design a system capable of forming a reversible and self-healing structure over the pH 4.5 to 7.5 range with a minimized mesh size that prevents the transport of infectious virions at the higher pH. We are also interested in understanding how temperature impacts the viscoelastic properties as well as the complex and shear viscosities as a function of the PBA to SHA ratio.

We have previously characterized PBA–SHA polymer networks formed from equal ratios of either 5 mol% or 10 mol% PBA and SHA functionalized HPMAm polymers.[5,17] Network formation depended on both pH and concentration with solid networks forming across the pH range of 5.5 to 7.5. For lower degrees of equal PBA and SHA functionalization, a higher polymer concentration was required to form transient networks at acidic pH. However, gels formed at neutral pH at 50 mg mL^{-1} polymer concentration. PBA_5–SHA_5 and PBA_{10}–SHA_{10} were transient networks and exhibited self-healing properties at pH 4.2, while only the PBA_5–SHA_5 material was capable of self-healing at pH 5.5. Above pH 5.5 the materials transitioned to brittle solid polymer networks that could be fractured and did not self-heal. The fact that at pH 5.5 the PBA_{10}–SHA_{10} gels were not self-healing, but PBA_5–SHA_5 formed a transient network indicates that the extent or number of crosslinks formed at a given pH impacts the ability of the gel to self-heal.[5] Qualitative investigations at concentrations lower than 50 mg mL^{-1} resulted in phase separation and no viscoelastic behaviour at either acidic or neutral pH. Here we report that decreasing the degree of polymer-bound PBA and polymer-bound SHA functionality to 1 mol% required 200 mg mL^{-1} of polymer to form weak PBA_1–SHA_1 transient networks even at pH 7.5. However, the resulting material could be cut into fragments that would rejoin in seconds to form a single cohesive mass. A series of rheological experiments were conducted to quantitatively evaluate the viscoelastic properties of the equal ratio of the PBA_1–SHA_1 polymer network (Fig. 1).

Dynamic rheology of PBA_1–SHA_1

The PBA_1–SHA_1 polymer network displays rheological behavior that is consistent with time-dependent dynamic gel networks.[27] The transient nature of the network is due to the reversible nature of the PBA–SHA complex. Fig. 1a illustrates the angular frequency dependence of the elastic modulus, G' and viscous modulus, G''. At low frequency G' increases, but is dominated by G''. At a critical frequency G'' reaches a maximum and G' reaches a plateau that exhibits weak frequency dependence. These results are in accord with other boronate–diol crosslinked systems as well as previous PBA–SHA crosslinked networks.[5,17,28,29] The fact that the G'' maximum is difficult to visualize and that G' does not dominate the G'' in the plateau region are in accord with reported results for weak transient networks formed from boronate crosslinks with polyalcohols.[28]

For the PBA_1–SHA_1 gel G' equals G'' at a frequency crossover of 2.5 rad s^{-1}. The inverse of this crossover frequency (in Hertz) determines the characteristic relaxation time, τ, of the crosslinked polymer network.[6,30] For networks utilizing a boronic acid–diol complex as the crosslink, τ describes the ensemble lifetime of the associations of the PBA–SHA moieties that then impacts the number of crosslinks formed at any given moment.[5,6,30–32]

For the PBA_1–SHA_1 network, the characteristic relaxation time is 1.6 s. Above the crossover frequency G' levels off and remains equal to G'' at approximately 10 Pa. The average of G' in this plateau region measures the dynamic strength of the polymer

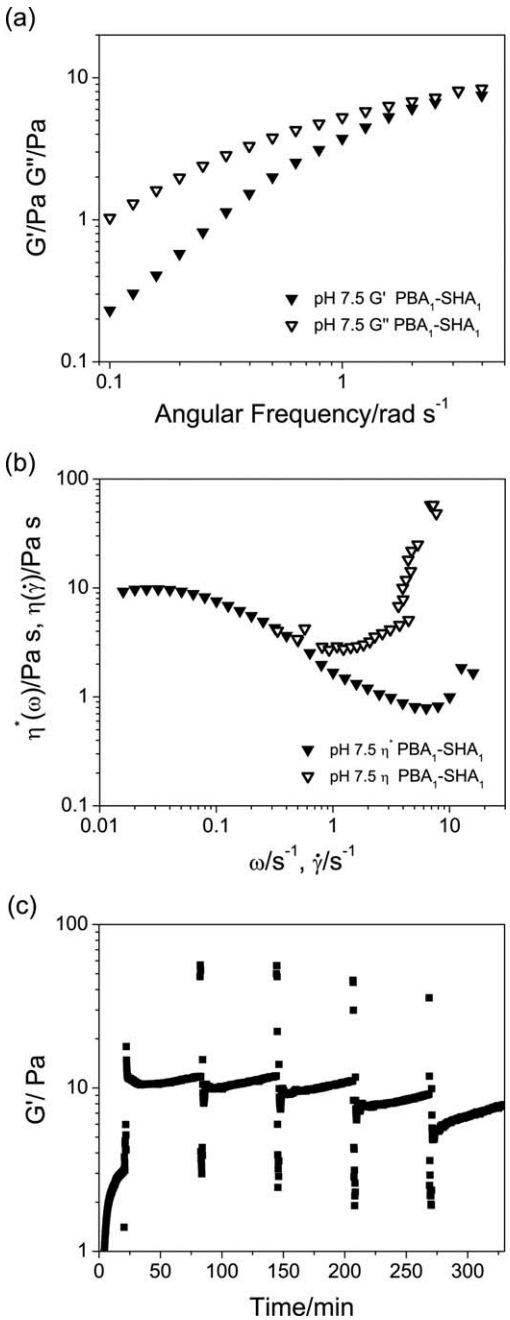

Fig. 1 Viscoelastic properties of $PBA_1 : SHA_1$ transient network formulated at 200 mg mL^{-1}, pH 7.5, 37 °C. (a) The elastic modulus, G' (closed), and loss modulus, G'' (open), versus frequency (ω) at an applied stress from the linear viscoelastic region. (b) Comparison of the simple viscosity, $\eta(\dot{\gamma})$ (open) and the complex viscosity, $\eta^*(\omega)$ (closed). (c) Recovery of gel's elastic strength, G', after a repeated break and recovery. $N = 3$, mean. Standard deviation has been removed to retain clarity of plots.

network, $G'_{plateau}$. The value of $G'_{plateau}$ depends on the number of crosslinks formed from the association of the reactive polymer-bound PBA and SHA moieties.[33] The dynamic viscosity or complex viscosity determined from the frequency sweeps displays a linear viscoelastic region at long time scales (low frequencies) that decreases at higher frequencies, rising slightly above 10 s^{-1} (Fig. 1b). The steady state viscosity was unstable at lower shear rates and rises sharply at a certain critical rate of shear, $\dot{\gamma} = 2\ s^{-1}$, with the viscosity increasing by over an order of magnitude. This shear thickening behavior has been observed for transient networks produced from boronate–diol crosslinks.[34]

To test the recoverability of the transient network structure an amplitude oscillatory stress above the linear viscoelastic region was applied for two minutes followed by a recovery period under small amplitude stress. The PBA_1–SHA_1 transient network at pH 7.5 displayed rapid recovery over five cycles of break and recovery (Fig. 1c). However, the $G'_{plateau}$ decreased slightly after each break cycle, additionally, the fact that the PBA_1–SHA_1 polymers did not form a transient network at pH 4.5 indicates that further optimization is required in order to apply these polymers as a microbicide gel.

pH dependence of gel formation

The parameters governing gelation for boronate–diol crosslinked networks strongly depend on the number of crosslinks formed and are thus impacted by any factor that affects the equilibrium of the boronate–diol complex. The formation of the stable tetrahedral PBA–SHA complex is highly pH dependent.[14] As pH decreases the PBA–SHA complex converts to the trigonal form and is rapidly hydrolyzed. We have found that decreasing the pH of a PBA–SHA network requires increasing either the polymer concentration or the degree of polymer functionalization in order to maintain transient networks that exhibit a region where G' is greater than or equal to G''. Similar behavior has been identified for the exothermic boronate–diol crosslinked networks where raising the temperature required an increase in the concentration of boronate ions to maintain a transient network.[28,29,35]

Qualitative observations revealed that the mixture of 200 mg mL^{-1} of PBA_1 and SHA_1 polymers formed only a viscous liquid at pH 4.5. Increasing the ratio of PBA moieties to SHA by combining 5 and 10 mol% PBA functionalized polymers with 1 mol% SHA functionalized polymers should increase the probability for PBA–SHA complexation at acidic pH formation and thus provide a transient extended network even at pH 4.5 The lower amount of SHA available for PBA to complex with will cap the number of PBA–SHA crosslinks capable of forming at pH 7.5 and thus allow preservation of the network's self-healing properties.

To quantitatively determine how pH and the ratio of polymer-bound PBA to polymer-bound SHA impacted the interaction between the two polymers we screened for transient network behavior as a function of pH at 200 mg mL^{-1} and 37 °C using video microscopy. This technique allows the determination of the ensemble-averaged mean squared displacement (MSD, $\langle \Delta r(t)^2 \rangle$, μm^2) by tracking multiple fluorescent particles within the polymer solutions.[20] Generally particles in viscous liquids diffuse freely, producing a linear relationship between the lag time, t, and the MSD (resulting in a slope of 1 in a log–log plot). In an elastic network the movement of the particles becomes constrained resulting in a plateau in the MSD (a slope near 0 in a log–log plot). This technique provides rapid screening of network properties with minimum amounts of material.[3]

We tracked fluorescently labeled 100 nm sulfate modified particles, similar in size to HIV-1 virions.[36] While the PBA_1–SHA_1

polymer network demonstrated a plateau in the MSD at pH 7.5, corresponding to the macrorheological properties of a transient network, low viscosity solutions were formed at pH's 4.5 and 5.5 (Fig. 2). Incorporation of a greater ratio of polymer-bound PBA to polymer-bound SHA reveals a decrease in the slope of the MSD, indicating the formation of extended polymer networks. From particle tracking at pH 4.5 it appears that the transient network formed by PBA_{10}–SHA_1 decreases the particle movement at shorter lag times than PBA_5–SHA_1, indicating a stronger network. Movement of the beads in the PBA_{10}–SHA_1 transient network at pH 7.5 is further reduced indicating that this network is indeed pH sensitive, and that the increasing pH further decreases the network mesh size as the PBA–SHA crosslink stabilizes and the maximum possible number of crosslinks formed. From the MSD the diffusion rate was determined and the average displacement of a 100 nm bead was calculated to be less than 1 μm in an hour. We have previously determined that the diffusion of these particles correlates with the transport of HIV-1 virions entrapped within PBA–SHA crosslinked polymer networks,[17] and thus the matrix formed from the PBA_{10}–SHA_1 at pH 7.5 indicates the potential to impede viral movement and thus act as a physical barrier to prevent transmission of HIV-1.[17]

Dynamic rheology of PBA_{10}–SHA_1 and PBA_5–SHA_1 transient networks—pH dependence

After determining that the polymer networks with a greater ratio of PBA to SHA formed gel networks, as demonstrated by a plateau in the MSD at pH 4.5, we then characterized the effect of pH, across the pH range of 4.5 to 7.5, has on their rheological properties. As can be seen in Fig. 3, the frequency curves of both the PBA_5–SHA_1 and PBA_{10}–SHA_1 polymer systems display time-dependent transient networks where the resulting moduli depend on both pH and ratio of PBA to SHA. Unlike the PBA_1–SHA_1 system, G' dominates G'' above the crossover frequency and the G'' is easily visualized. Greater pH sensitivity occurred below pH 6.5. At pH 4.5 we were unable to determine a linear viscoelastic region for the PBA_5–SHA_1 system and could not obtain frequency sweep data even though particle tracking indicated formation of a transient network. However the PBA_{10}–SHA_1 system formed a transient network with a characteristic relaxation time of 1 s and a $G'_{plateau}$ of 130 Pa (see Fig. S1†). At pH 5.5 transient networks formed with both unequal PBA to SHA ratios. At this pH the ratio of the PBA to SHA appears to impact the extent of PBA–SHA complex formation and thus the

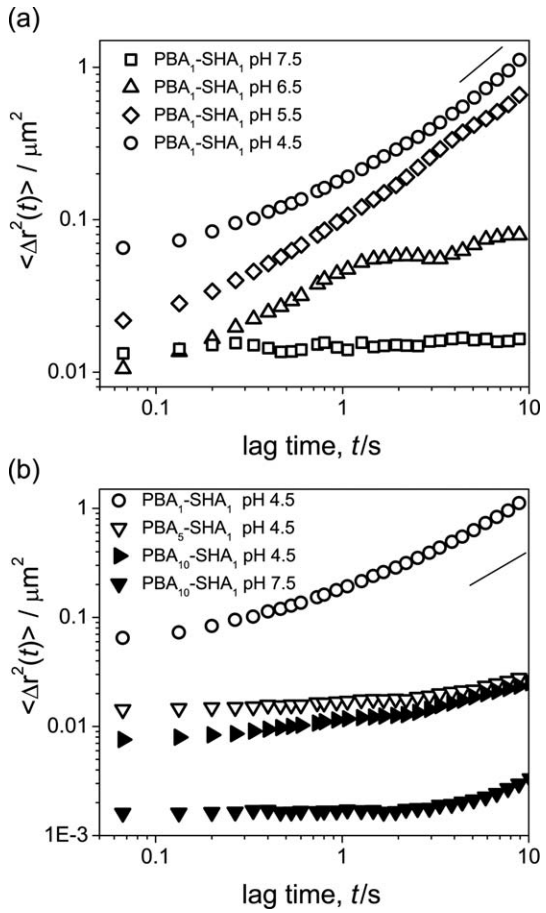

Fig. 2 Ensemble-averaged mean squared displacement for 100 nm fluorescent labeled sulfonated particles at 37 °C moving in (a) the PBA_1–SHA_1 polymer network as a function of pH and (b) at pH 4.5 as a function of the ratio of polymer-bound PBA to polymer-bound SHA. The solid line depicts a slope of 1 and indicates where diffusive behavior occurs.

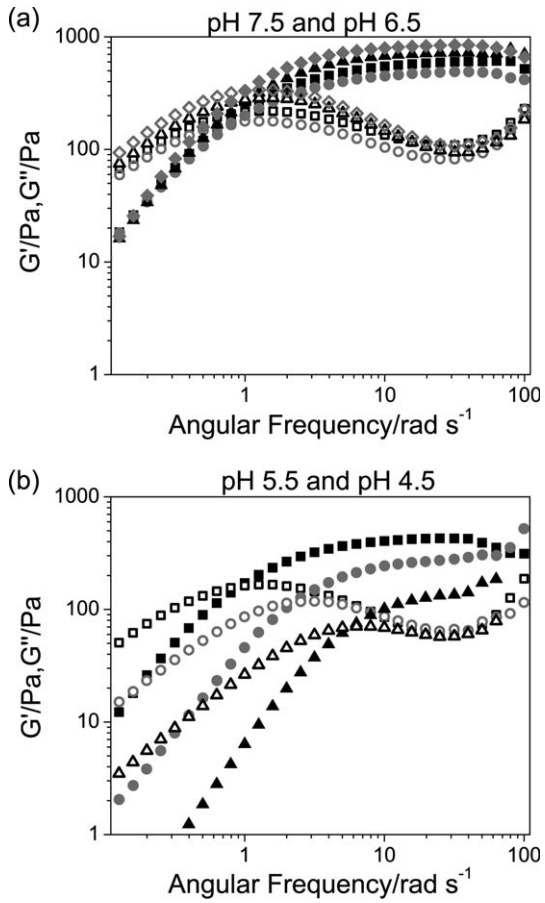

Fig. 3 Comparison of the elastic modulus, G' (closed) and loss modulus, G'' (open) for transient networks formed from unequal ratios of functionalized PBA to SHA polymers at 200 mg mL^{-1} and 37 °C as a function of pH. (a) pH 7.5 and pH 6.5 for PBA_{10} : SHA_1 and PBA_5 : SHA_1, and (b) pH 5.5 for PBA_{10} : SHA_1 and PBA_5 : SHA_1 and at pH 4.5, only PBA_{10} : SHA_1. $N = 3$, mean.

ensemble lifetime of the transient networks' crosslinks and overall dynamic network strength. The PBA_{10}–SHA_1 system exhibits a stronger transient network with a higher characteristic relaxation time of 5.3 s compared to 2.6 s for PBA_5–SHA_1 and corresponding $G'_{plateau}$'s of 552 Pa and 258 Pa respectively.

Above pH 5.5, pH and the ratio of PBA to SHA appear to have only a gradual effect on the ensemble lifetime of the crosslinks and the network strength for the PBA_{10}–SHA_1 system. The increase in pH from 5.5 to 6.5 appears to modify both the τ and $G'_{plateau}$ for the PBA_5–SHA_1 polymer network. At and above pH 6.5 the PBA_5–SHA_1 and PBA_{10}–SHA_1 materials displayed similar viscoelastic properties with only a gradual increase in τ and a leveling off of $G'_{plateau}$ as the angular frequency increased (see Fig. S1†).

We superimposed the frequency sweeps at each pH of the PBA_1–SHA_1, PBA_5–SHA_1 and PBA_{10}–SHA_1 networks to validate whether a common relaxation mechanism was responsible at each condition (Fig. 4). This was done by shifting the frequency curves horizontally and vertically so that all curves combined on the reference curve (PBA_{10}–SHA_1, pH 7.5, 37 °C) (see Table S1†). The frequency sweep curve for both moduli of the PBA_1–SHA_1 system at pH 7.5 could be superimposed below the composite crossover frequency, but G' and G'' above this frequency could not be shifted to match the composite curves of the PBA_5–SHA_1 and PBA_{10}–SHA_1 polymer networks and is thus not shown in Fig. 4. In comparison the PBA_5–SHA_1 and PBA_{10}–SHA_1 transient networks exhibit good superposition in the terminal region.

These results suggest that a different relaxation mechanism may exist in the weak symmetrically crosslinked PBA_1–SHA_1 mixture compared to the transient networks where the PBA to SHA ratio is larger. The superposition of the PBA_5–SHA_1 and PBA_{10}–SHA_1 moduli curves indicates that in these networks the same relaxation mechanism occurs. Deviation was exhibited at longer frequencies, a phenomenon that has been observed for other boronate–diol crosslinked systems.[6,28,37] Large vertical shift factors were required to attempt to fit the PBA_1–SHA_1 at pH 7.5 as well as the PBA_{10}–SHA_1 at pH 4.5 indicating the lower degree of crosslinking occurring in these samples. All other vertical shift factors were close to 1 indicating that the association between PBA and SHA does not change the intrinsic mesh size of the transient network as the pH decreases.[33]

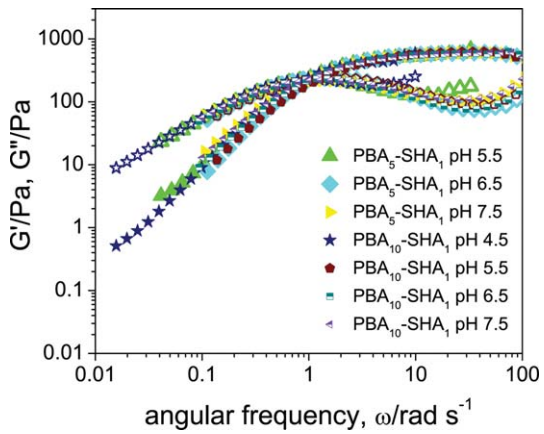

Fig. 4 Master curve analysis of G' (closed, or upper half closed) and G'' (open, or bottom half closed) for PBA_5–SHA_1 and PBA_{10}–SHA_1 at each pH shifted to superimpose onto the reference curve, PBA_{10}–SHA_1, pH 7.5, 37 °C. a_T and b_T are the horizontal and vertical shift factors, respectively. The frequency sweep curves for the PBA_1–SHA_1 transient network at pH 7.5 could not be superimposed to match the vertical shifts for G' and G'' above the master crossover frequency and is not displayed. The mean moduli of triplicate samples were used for both the reference curve and the curves to be shifted.

Considering that the boron-11 NMR data collected by Stolowitz *et al.* suggested that the majority of PBA at pH 7.5 existed in the tetrahedral PBA–SHA complex,[14] we anticipated that increasing the ratio of PBA compared to SHA would not dramatically impact τ or $G'_{plateau}$ at this pH. However, both the PBA_5–SHA_1 and PBA_{10}–SHA_1 systems exhibited an increase in both parameters compared to the PBA_1–SHA_1 mixture at pH 7.5. The characteristic relaxation time increased only slightly from 4 s to approximately 7 s suggesting that the higher ratio of PBA to SHA only marginally impacts the ensemble average lifetime of the crosslinks. However $G'_{plateau}$ increased more than sixty times indicating that while the ensemble lifetime remains relatively unaffected, the number of crosslinks has increased. The ratio of G'' to G' ($\tan\delta$) also decreased from approximately 1 to 0.4 ($\omega = 4$ rad s^{-1}) in the PBA_1–SHA_1 materials compared to the PBA_5–SHA_1 and PBA_{10}–SHA_1 transient networks, indicating an increase in elastic behavior. These results imply that even at pH 7.5 the higher probability of crosslink formation due to an increased ratio of PBA to SHA moieties impacts the density of crosslinking and dynamic network strength. It is likely that the rate of hydrolysis of the PBA–SHA complex occurs more extensively than we anticipated. We hypothesize that as the PBA–SHA complex is hydrolyzed the increased ratios of PBA to SHA dramatically improve the probability of forming new crosslinks in a given time frame, thus increasing the extent of crosslinking and dynamic network strength overall at pH 7.5.

Dynamic rheology of PBA_{10}–SHA_1 and PBA_5–SHA_1 transient networks—temperature dependence

Due to the exothermic nature of the boronate–diol bond we were also interested in determining how temperature impacted the dynamic viscoelastic properties of PBA_1–SHA_1, PBA_{10}–SHA_1 and PBA_5–SHA_1 transient networks. Dynamic frequency sweeps were performed from 10 °C to 55 °C at pH 7.5. Water was added to the solvent trap of the geometry and a cover was sealed to the Peltier plate with vacuum grease to create a humid environment and prevent dehydration of the aqueous polymer networks. This pH was chosen to ensure that a transient network formed at higher temperatures to ensure datasets with more than three data points. A time-temperature superposition was obtained using shift factors (Fig. 5). PBA_5–SHA_1 and PBA_{10}–SHA_1 at pH 7.5, 25 °C reveal a reduced fit below the crossover frequency while above the crossover frequency G' and G'' superimposed. The poor fit may be attributed to the increased τ, over 90 s, thus indicating the transition from a transient network to the formation of a solid network in comparison to the reference curve. The PBA_1–SHA_1 network shows a good fit in the terminal region below the master curve crossover frequency. However, only the G'' moduli curves at 10 °C fit above this point. Other boronate–diol gels show similar deviations of G'' in materials at low pH's or high temperatures in superpositions to

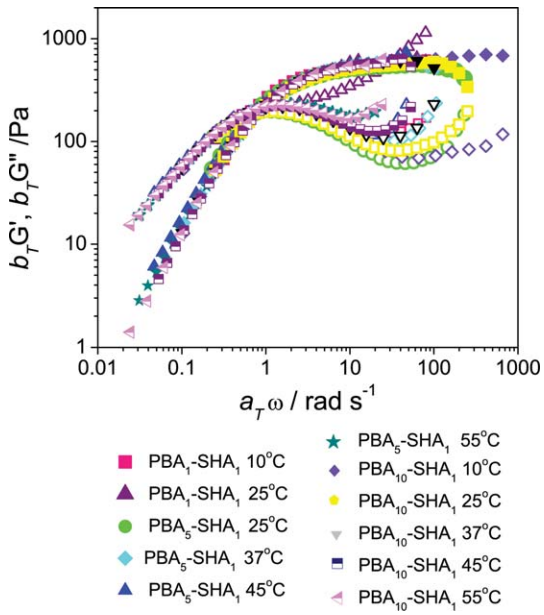

Fig. 5 Time-temperature superposition of G' (closed or upper half closed) and G'' (open or bottom half closed) of PBA$_1$–SHA$_1$, PBA$_5$–SHA$_1$ and PBA$_{10}$–SHA$_1$ transient networks at pH 7.5 using shift factors to create a composite curve to the reference frequency sweep curve of PBA$_{10}$–SHA$_1$, pH 7.5, 37 °C. Above 25 °C G' and G'' for the PBA$_1$–SHA$_1$ crosslinked network could not be superimposed above the master crossover frequency and are not displayed.

a reference curve.[28] This behavior has been observed in other associating polymers where the increase in G'' is an indication of a second relaxation mechanism.[39] This result demonstrates that the same relaxation mechanism occurs in both the PBA$_1$–SHA$_1$ as the PBA$_5$–SHA$_1$ and PBA$_{10}$–SHA$_1$ transient networks, especially under the stronger PBA–SHA interaction conditions of lower temperatures and higher pH, which was not clear in the pH superposition curve. The minimal changes in the vertical shift factors, except for the PBA$_1$–SHA$_1$ networks above 10 °C, indicate that the PBA–SHA complexation minimally impacts the network mesh size with increasing temperature. However, the large horizontal shift factors reveal that the time scales of these interaction changes are impacted by the temperature (see Table S2†).[33]

As suggested by the propensity for G'' to increase above the crossover frequency, we found that the frequency sweep curves could not be approximated by a Maxwell model with a single relaxation mode at any of the pH and temperature conditions tested. The individual frequency sweeps could more accurately be represented by modeling with the presence of two relaxation modes.[29,38] However even for these fits only the elastic modulus showed R^2 values near 1. The viscous modulus frequency sweeps were modeled poorly. The presence of a second relaxation mode has been exhibited by other boronic acid crosslinked systems.[29] We hypothesize that the rapid climb in G'' after the crossover frequency is due to the second shorter relaxation mechanism, likely attributed to polymer entanglements, that begins to dominate the viscoelastic behavior as the rate of dissociation of the PBA–SHA complex becomes larger than the association rate and few crosslinks are formed. This behavior has also been observed in other associating polymers.[39]

Steady shear viscosity and complex viscosity

The impact of pH and the greater ratio of PBA to SHA on the polymer networks' complex viscosity, $\eta^*(\omega)$, and steady state flow viscosity, $\eta(\dot{\gamma})$, were also characterized for comparison (Fig. 6). The majority of semi-solid topical gel formulations are weakly associated polymer systems that exhibit shear thinning behavior above shear rates of 0.01 s^{-1} with some materials exhibiting Newtonian behavior below 0.01 s^{-1} under steady state flow.[40,41] Here, both $\eta^*(\omega)$ and $\eta(\dot{\gamma})$ for the PBA$_5$–SHA$_1$ and PBA$_{10}$–SHA$_1$ networks exhibit Newtonian behavior below shear rates of approximately 1 s^{-1}.

The rapid shear thickening, observed as the increase in $\eta(\dot{\gamma})$ above a critical shear rate, is also not observed in the polymer networks with a greater PBA to SHA stoichiometry ratio. However, a mild shear thickening behavior does transpire with decreasing pH. Below pH 6.5 a slight increase in $\eta(\dot{\gamma})$ occurred at shear rates above 0.7 s^{-1}. Above pH 6.5 $\eta(\dot{\gamma})$ remains level until approximately 1 s^{-1}. Above 1 s^{-1} the flow became unstable, a phenomenon exhibited by poly(vinyl alcohol)–sodium borate polymer complexes,[34] impeding our ability to quantitatively determine behavior at higher shear rates. We did observe that after exposure to high shear rates clumps of the crosslinked material could be found in various locations outside the geometry. Likely the samples shear thinned rapidly and were

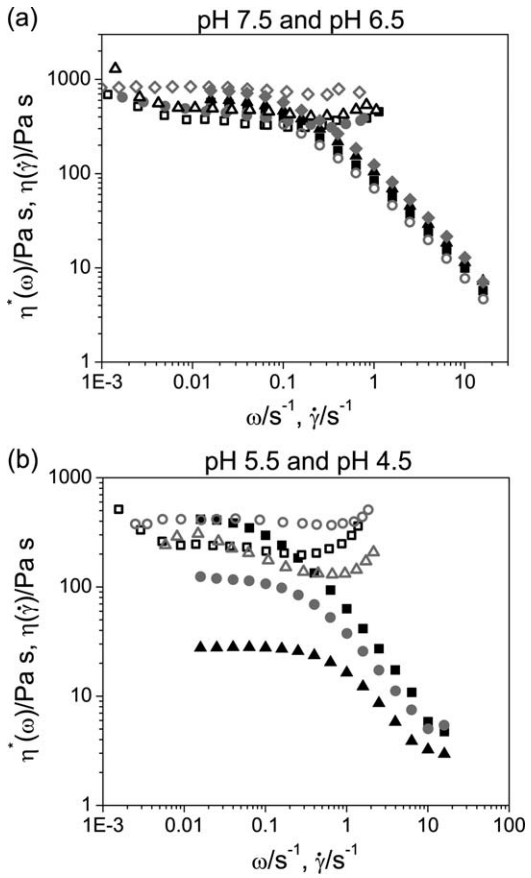

Fig. 6 Comparison of the simple viscosity $\eta(\dot{\gamma})$ (open) and complex viscosity $\eta^*(\omega)$ (closed) for networks formed from PBA$_{10}$: SHA$_1$ and PBA$_5$: SHA$_1$ polymer networks at (a) pH 7.5 and 6.5 and (b) pH 5.5 and 4.5 (10 : 1 only). $N = 3$, mean.

ultimately spun out from the geometry. Shear thinning behavior was recorded in the PBA_{10}–SHA_1 transient network at 10 °C using a very long equilibration time (data not shown).

Only slight decreases in the value of $\eta(\dot{\gamma})$ in the plateau region occurred with decreasing pH compared to $\eta^*(\omega)$. The dramatic deviation of $\eta(\dot{\gamma})$ from $\eta^*(\omega)$ below pH 6.5 suggests that different microstructure states exist in the dynamic and steady state.[42] Above pH 6.5 $\eta(\dot{\gamma})$ agrees with $\eta^*(\omega)$ at low $\dot{\gamma}$ where $\eta(\dot{\gamma})$ is independent of $\dot{\gamma}$, in agreement with the Cox–Merz rule.[43] Then $\eta(\dot{\gamma})$ maintains its plateau while $n^*(\omega)$ decreases. This behavior has been exhibited for previous boronate–diol systems but with a much greater increase in $\eta(\dot{\gamma})$ occurring upon divergence from $\eta^*(\omega)$.[34]

The observed dependence of shear thickening behavior on pH and ratio of polymer-bound PBA to polymer-bound SHA is interesting. Shear thickening behavior implies that an increase in the lifetime and/or number of crosslinks is impacted by flow.[37,44] It has been hypothesized that crosslinking between diol–boronate complexes may be impacted by polymer chain orientation. Potentially an increase in the flow allows more parallel orientation of the polymer chains which could create favorable alignment for increasing association between polymer-bound PBA and SHA on adjacent chains.[37] The decrease in the magnitude of shear thickening appears to correlate with increasing dynamic network strength. Similar behavior has been observed for telechelic associating polymers.[42] The minimal change from unity in the vertical shift factors for both the pH and temperature superposition curves, as well as the trend in the stabilization of the dynamic network strength at higher pH, suggest that the majority of the SHA moieties are complexed with PBA in the PBA_5–SHA_1 and PBA_{10}–SHA_1 transient networks above pH 6.5. Thus modification in alignment of the polymer chains under flow would likely not impact the number of crosslinks formed in a system where the maximum number of associations between PBA and SHA molecules already existed. Thus no shear thickening behavior would be observed. In the weaker systems where the number of crosslinks is not maximized, alignment of the polymer chains under flow could allow for improved steric interactions and increase number of PBA–SHA associations resulting in shear thickening behavior. This hypothesis would explain the larger degree of shear thickening exhibited by the PBA_{10}–SHA_1 gel at pH 4.5 and the PBA_1–SHA_1 gel at pH 7.5 but not in the stronger networks.

Self-healing properties of transient networks formed with PBA_{10}–SHA_1 stoichiometry

For biomedical applications at physiological pH, where the system may be exposed to high shears or stresses, these materials may need to self-heal at neutral pH. We were interested in assessing if the increase in the number of crosslinks at neutral pH compared to the PBA_1–SHA_1 material impacted self-healing behavior. We also characterized the self-healing ability at pH 4.5. Qualitative observations of the PBA_{10}–SHA_1 crosslinked network at both pH's revealed the ability to heal after being cut into pieces. To quantitatively test the recoverability of the transient networks, dynamic rheology was utilized by measuring the recovery of the associating polymers under linear viscoelastic conditions after a 2 min exposure to high oscillatory stress. The oscillatory stress was chosen just beyond the linear viscoelastic region to result in approximately a 50% decrease in G' after two minutes. We tested a range of higher stresses and found that while transient networks reformed they would have spun out from underneath the geometry thus hampering accurate measurements of the recovery. Similar behavior occurred when exposing the associating polymers to shear rates of 100 s^{-1} for two minutes. Because the transient networks will likely endure repeated disruptions in their network structure a series of five breaks followed by a 60 minute recovery period were measured (Fig. 7).

At both pH's the PBA_{10}–SHA_1 transient networks recovered from the applied stress. A slight loss in the elastic modulus occurred for the pH 4.5 samples after the first two breaks followed by stabilization of the elastic modulus. At pH 7.5 the gel showed a slight loss in G' after each successive break. The pH 4.5 sample recovered to a maximum value of G' more rapidly than the pH 7.5 transient network. This is likely due to the fewer crosslinks and shorter ensemble lifetime as determined from dynamic rheology than those exhibited by the pH 7.5 network. While the number of crosslinks increased in the PBA_{10}–SHA_1

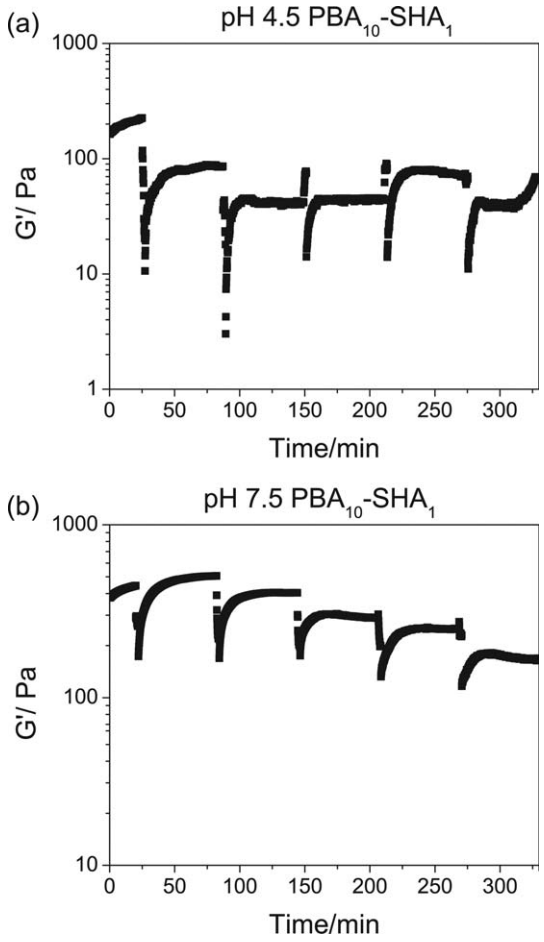

Fig. 7 The stress recovery of PBA_{10}–SHA_1 transient network after five cycles of recovery from stress-induced breakdowns at pH 4.5 and 7.5. An oscillatory stress above the linear viscoelastic region was applied for 2 min followed by linear recovery measurements (25 Pa oscillatory stress, 5 rad s^{-1}). (a) Recovery of the PBA_{10}–SHA_1 transient network at pH 4.5 and (b) at pH 7.5.

system at pH 7.5 compared to the equally crosslinked PBA_1–SHA_1 associating polymer, the ability to cap the maximum number of crosslinks through unequal ratios yielded a transient network capable of self-healing at pH 7.5.

Conclusions

Manipulating the degree of crosslinking in a PBA–SHA associating polymers by combining ratios of PBA_{10} with SHA_1 circumvents issues in creating structures capable of self-healing after exposures to stress at pH 7.5 by forming an extended transient network at pH 4.5 to pH 7.5. This approach unlike the materials using a 5 : 5 or 10 : 10 stoichiometry described previously by us, allows the development of transient networks whose viscoelastic properties can be modulated to form a viscoelastic material at slightly acidic pH with the ability to prevent stress or shear induced trauma to the crosslinked polymer matrix at pH 7.5. We therefore believe the unequal stoichiometry of polymer-bound PBA to polymer-bound SHA provides a unique approach to controlling the viscoelastic properties of a pH responsive reversible crosslinked network. This work reveals the flexibility of the PBA–SHA complex to be exploited for pH responsive drug delivery applications through the intelligent design of material properties. Molecular engineering approaches thus provide the possibility to develop improved materials for biological and other applications.

Acknowledgements

Funded by a grant from the Bill & Melinda Gates Foundation through the Grand Challenges Exploration Initiative (P.K.), NIH, grant number R21-AI062445 (P.K.), and a University of Utah Graduate Fellowship (J.J.)

Notes and references

1 A. P. Nowak, V. Breedveld, L. Pakstis, B. Ozbas, D. J. Pine, D. Pochan and T. J. Deming, *Nature*, 2002, **417**, 424–428.
2 S. Ramachandran, Y. Tseng and Y. B. Yu, *Biomacromolecules*, 2005, **6**, 1316–1321.
3 C. Xu, V. Breedveld and J. Kopecek, *Biomacromolecules*, 2005, **6**, 1739–1749.
4 Y. Zhao, H. Yokoi, M. Tanaka, T. Kinoshita and T. Tan, *Biomacromolecules*, 2008, **9**, 1511–1518.
5 M. C. Roberts, M. C. Hanson, A. P. Massey, E. A. Karren and P. F. Kiser, *Adv. Mater.*, 2007, **19**, 2503–2507.
6 M. C. Roberts, A. Mahalingam, M. C. Hanson and P. F. Kiser, *Macromolecules*, 2008, **41**, 8832–8840.
7 E. Pezron, A. Ricard, F. Lafuma and R. Audebert, *Macromolecules*, 1988, **21**, 1121–1125.
8 S. D. Bergman and F. Wudl, *J. Mater. Chem.*, 2008, **18**, 41–62.
9 B. J. Adzima, H. A. Aguirre, C. J. Kloxin, T. F. Scott and C. N. Bowman, *Macromolecules*, 2008, **41**, 9112–9117.
10 S. K. Kundu, T. Matsunaga, M. Yoshida and M. Shibayama, *J. Phys. Chem. B*, 2008, **112**, 11537–11541.
11 D. M. Loveless, S. L. Jeon and S. L. Craig, *Macromolecules*, 2005, **38**, 10171–10177.
12 P. S. Russo, in *ACS Symposium Series*, 1987, vol. 350, pp. 1–21.
13 G. Springsteen and B. Wang, *Tetrahedron*, 2002, **58**, 5291–5300.
14 M. L. Stolowitz, C. Ahlem, K. A. Hughes, R. J. Kaiser, E. A. Kesicki, G. Li, K. P. Lund, S. M. Torkelson and J. P. Wiley, *Bioconjugate Chem.*, 2001, **12**, 229–239.
15 J. P. Wiley, K. A. Hughes, R. J. Kaiser, E. A. Kesicki, K. P. Lund and M. L. Stolowitz, *Bioconjugate Chem.*, 2001, **12**, 240–250.
16 B. Rihova, M. Bilej, V. Vetvicka, K. Ulbrich, J. Strohalm, J. Kopecek and R. Duncan, *Biomaterials*, 1989, **10**, 335–342.
17 J. I. Jay, S. Shukair, K. Langheinrich, T. J. Johnson, M. R. Clark, T. J. Hope and P. F. Kiser, *Adv. Funct. Mater.*, 2009, **19**, 2969–2977.
18 J. Buchert, T. Tamminen and L. Viikari, *J. Biotechnol.*, 1997, **57**, 217–222.
19 N. D. Winblade, I. D. Nikolic, A. S. Hoffman and J. A. Hubbell, *Biomacromolecules*, 2000, **1**, 523–533.
20 J. C. Crocker and D. G. Grier, *J. Colloid Interface Sci.*, 1996, **179**, 298–310.
21 B. Cutler and J. Justman, *Lancet Infect. Dis.*, 2008, **8**, 685–697.
22 R. A. Cone, *Adv. Drug Delivery Rev.*, 2009, **61**, 75–85.
23 D. H. Owen, J. J. Peters, M. L. Lavine and D. F. Katz, *Contraception*, 2003, **67**, 57–64.
24 M. L. Stolowitz, C. Ahlem, K. A. Hughes, R. J. Kaiser, E. A. Kesicki, G. Li, K. P. Lund, S. M. Torkelson and J. P. Wiley, *Bioconjugate Chem.*, 2001, **12**, 229–239.
25 H. Okada and A. M. Hillery, in *Drug Delivery and Targeting*, ed. A. M. Hillery, A. W. Lloyd and J. Swarbrick, Taylor and Francis Inc, NY, 1st edn, 2001, ch. 11, pp. 306–307.
26 C. Tevi-Benissan, L. Belec, M. Levy, V. Schneider-Fauveau, A. Si Mohamed, M. C. Hallouin, M. Matta and G. Gresenguet, *Clin. Diagn. Lab. Immunol.*, 1997, **4**, 367–374.
27 R. P. Sijbesma, F. H. Beijer, L. Brunsveld, B. J. B. Folmer, J. H. K. K. Hirschberg, R. F. M. Lange, J. K. L. Lowe and E. W. Meijer, *Science*, 1997, **278**, 1601–1604.
28 E. Pezron, A. Ricard and L. Leibler, *J. Polym. Sci., Part B: Polym. Phys.*, 1990, **28**, 2445–2461.
29 K. Koga, A. Takada and N. Nemoto, *Macromolecules*, 1999, **32**, 8872–8879.
30 I. D. Robb and J. B. A. F. Smeulders, *Polymer*, 1997, **38**, 2165–2169.
31 E. Pezron, A. Ricard, F. Lafuma and R. Audebert, *Macromolecules*, 1988, **21**, 1121–1125.
32 R. K. Schultz and R. R. Myers, *Macromolecules*, 1969, **2**, 281–285.
33 S. Kesavan and R. K. Prud'homme, *Macromolecules*, 1992, **25**, 2026–2032.
34 T. Inoue and K. Osaki, *Rheol. Acta*, 1993, **32**, 550–555.
35 E. Pezron, L. Leibler, A. Ricard and R. Audebert, *Macromolecules*, 1988, **21**, 1126–1131.
36 M. Gentile, T. Adrian, A. Scheidler, M. Ewald, F. Dianzani, G. Pauli and H. R. Gelderblom, *J. Virol. Methods*, 1994, **48**, 43–52.
37 N. Ide, T. Sato, T. Miyamoto and T. Fukuda, *Macromolecules*, 1998, **31**, 8878–8885.
38 M. C. Roberts, PhD thesis, University of Utah, 2008.
39 J.-F. Le Meins and J.-F. Tassin, *Colloid Polym. Sci.*, 2003, **281**, 283–287.
40 J. Das Neves, M. V. Da Silva, M. P. Goncalves, M. H. Amaral and M. F. Bahia, *Curr. Drug Delivery*, 2009, **6**, 83–92.
41 A. Mahalingam, E. Smith, J. Fabian, F. R. Damian, J. J. Peters, M. R. Clark, D. Friend, D. F. Katz and P. F. Kiser, *Pharm. Res.*, 2010, **27**, 2478–2491.
42 B. Kaffashi, M. Barmar and J. Eyvani, *Colloids Surf., A*, 2005, **254**, 125–130.
43 W. P. Cox and E. H. Merz, *J. Polym. Sci.*, 1958, **28**, 619–622.
44 L. Choplin and J. Sabatié, *Rheol. Acta*, 1986, **25**, 570–579.